

Molecular Dynamics Integration Time Step Dependence of the Split Integration Symplectic Method on System Density

Dušanka Janežič* and Matej Praprotnik

National Institute of Chemistry, Hajdrihova 19, 1000 Ljubljana, Slovenia

Received July 17, 2003

This paper shows that the maximal size of the integration time step of the Split Integration Symplectic Method (SISM) for molecular dynamics (MD) integration, a combination of the analytical solution of the high-frequency harmonic part of the Hamiltonian and the numerical solution of the low-frequency remaining part, depends on the system density. This approach was tested on a system of linear chain molecules. The numerical results indicate that the integration time step used by the SISM is limited by atoms' motion generated by the electrostatic and Lennard-Jones interactions in the system. As the density of the system increases, the size of the integration time step allowed by the SISM thus becomes smaller but remains significantly larger than possible by standard methods of the same order and complexity.

1. INTRODUCTION

Molecular dynamics (MD) simulation is a widely used computational method for simulating the physical properties of complex molecular systems.¹ For each atom of the system, the Hamilton equations of motion are integrated to compute the particles' trajectories in phase space, which is composed of the coordinates and momenta of all the particles. To perform an MD simulation of a system with a finite number of degrees of freedom, the Hamilton equations of motion

$$\frac{dp_i}{dt} = -\frac{\partial H}{\partial q_i}, \quad \frac{dq_i}{dt} = \frac{\partial H}{\partial p_i} \quad i = 1 \dots d \quad (1)$$

are solved, where H is the Hamiltonian, q_i and p_i are the coordinate and momentum, respectively, and d is the number of degrees of freedom. The MD simulation thus provides an insight into the microscopic behavior of complex molecular systems. These systems, which are studied by MD simulation, are in the class of classical many-body problems. The analytical solution usually does not exist for these dynamical systems, and a number of MD algorithms for finding the numerical solution have been proposed.^{2–7} A major obstacle in the development of efficient algorithms to propagate numerical trajectories of complex molecular systems is that these Hamiltonian systems consist of both fast and slow degrees of freedom. Because the fastest degrees of freedom in the system limit the size of the allowed integration time step in standard methods, studying processes that are several orders of magnitude longer than the fastest motion in the system is difficult despite growing CPU power. Therefore, MD simulation algorithms that allow the use of larger integration time steps are required. Due to their property of conserving a system's energy, the symmetric and symplectic integrators, which are also time reversible, are a suitable choice in achieving this goal.⁸

A new efficient symplectic integration algorithm for MD simulations of isolated linear molecules using the splitting

of the total Hamiltonian into the high-frequency harmonic and low-frequency remaining part was first introduced in ref 9. It was assumed there that bond stretching satisfactorily describes all vibrational motions of a molecule. The vibrational motion, which was described by the high-frequency harmonic part of the Hamiltonian, was solved analytically with the aid of the normal coordinates. In ref 10 the method devised in ref 9 was extended to also treat systems of linear molecules. The generalization of this symplectic method was first introduced in ref 11. The crucial difference from the approach described in refs 9 and 10 was that normal modes with frequency zero were used for describing the rotational and translational motion of molecules. This approach was also extended to a system of linear molecules for which it can be assumed that both bond stretching and angle bending satisfactorily describe all vibrational motion of molecules. The performance and the properties of the method, such as the maximal allowed integration time step, have not yet been fully explored.

In this article, which builds upon ref 11, a study of integration time step dependence on the system density for SISM^{11,12} for MD integration, which combines the analytical solution of the high-frequency harmonic part of the Hamiltonian and the numerical solution of the remaining part, is presented. Because the high-frequency degrees of freedom are treated analytically, i.e., independently of the size of the integration time step, the SISM can employ a significantly larger integration time step size than can be used by the standard leapfrog Verlet (LFV) method.¹³

2. METHODOLOGY

The SISM, which is schematically presented in Figure 1, is derived in terms of the Lie algebraic language. The Hamilton equations 1 can be written in the form

$$\frac{dx}{dt} = \{x, H\} = \hat{L}_H x \quad (2)$$

where \hat{L}_H is the Poisson bracket operator and $x = (q, p)$ is a

* Corresponding author e-mail: dusa@cmm.ki.si.

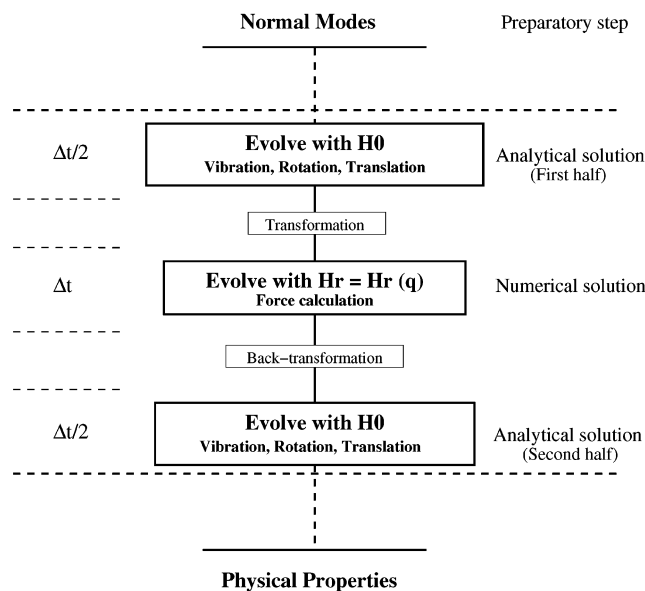


Figure 1. Solution scheme for SISM.

vector of the coordinates and momenta of all the particles. The formula

$$\mathbf{x}|_{t+\Delta t} = \exp(\Delta t \hat{L}_H) \mathbf{x}|_t \quad (3)$$

is the formal solution of the Hamiltonian system (2) in terms of Lie operators and represents the exact time evolution of a trajectory in phase space from t to $t+\Delta t$, where Δt is the integration time step.¹⁴ Symplectic integration replaces $\exp(\Delta t \hat{L}_H)$ by a product of symplectic maps that approximate $\exp(\Delta t \hat{L}_H)$ to a given order.⁸

We split the Hamiltonian H into two parts⁹

$$H = H_0 + H_r \quad (4)$$

where H_0 is the pure harmonic part and H_r is the remaining part of the total Hamiltonian.

Then the following second-order approximation, known as the generalized leapfrog scheme,¹⁵ can be used in (3)

$$\mathbf{x}|_{t+\Delta t} \approx \exp\left(\frac{\Delta t}{2} \hat{L}_{H_0}\right) \exp(\Delta t \hat{L}_{H_r}) \exp\left(\frac{\Delta t}{2} \hat{L}_{H_0}\right) \mathbf{x}|_t \quad (5)$$

This describes how to propagate from one point in phase space to another. First, the system is propagated for a half integration time step by H_0 , then for a whole step by H_r , and finally for another half step by H_0 . The whole integration time step thus combines the analytical evolution of H_0 with a correction arising from the H_r performed by numerical integration. This integration scheme was used as the basis for the development of the SISM which reads for each molecule in the system as follows:

• **Preparatory step:** at the outset of calculation, vibrational frequencies and normal modes of H_0 , represented by the normal coordinates P_i, Q_i ($i = 1, \dots, 3N$), are determined. The initial normal coordinates are obtained from the initial atoms' velocities and the initial displacements of the atoms from their equilibrium positions by means of the transformational matrix A . The columns of A are the eigenvectors of the Hessian, the root-mass-weighted second derivative

matrix of the bond stretching and angle bending part of the potential function.¹⁶ N is the number of atoms in each molecule.

• **Analytical solution** [propagation by $\exp(\Delta t/2 \hat{L}_{H_0})$]: the normal coordinates at the beginning of the integration step, P_i^0, Q_i^0 , are rotated in phase space by the corresponding vibrational frequency ω_i for $\Delta t/2$:

$$\begin{bmatrix} P_i' \\ Q_i' \end{bmatrix} = \mathbf{R} \begin{bmatrix} P_i^0 \\ Q_i^0 \end{bmatrix} \quad (6)$$

$$\mathbf{R} = \begin{bmatrix} \cos(\omega_i \Delta t/2) & -\omega_i \sin(\omega_i \Delta t/2) \\ (1/\omega_i) \sin(\omega_i \Delta t/2) & \cos(\omega_i \Delta t/2) \end{bmatrix} \quad (7)$$

where $\omega_i \neq 0$ defines the vibrations of atoms in each molecule and $\omega_i = 0$ defines translations and rotations of molecules. The normal coordinates of the normal modes with frequency zero ($\lim_{x \rightarrow 0} \sin x/x = 1$ for $\omega_i = 0$) evolve as

$$P_i' = P_i^0 \quad (8)$$

$$Q_i' = P_i^0 \frac{\Delta t}{2} + Q_i^0 \quad (9)$$

Coordinate transformation: the normal coordinates P_k', Q_k' are transformed to the Cartesian displacement coordinates $\Delta p_k', \Delta q_k'$ (m_i are the atoms' masses):

$$\Delta p_k' = \sqrt{m_i} \sum_k A_{ik} P_k' \quad (10)$$

$$\Delta q_k' = \frac{1}{\sqrt{m_i}} \sum_k A_{ik} Q_k' \quad (11)$$

• **Numerical solution** [evolution by $\exp(\Delta t \hat{L}_{H_r})$]: momenta in the Cartesian coordinates are numerically integrated

$$p_i'' = p_i' - \Delta t \left(\frac{\partial H_r}{\partial q} \right) \quad (12)$$

$$q_i'' = q_i' + \Delta t \left(\frac{\partial H_r}{\partial p} \right) = q_i' \quad (13)$$

Only one force calculation per integration step must be performed. Since $H_r = H_r(q)$ and $(\partial H_r / \partial p) = 0$, only momenta change in this part.

Back-transformation: the Cartesian displacement coordinates $\Delta p_k'', \Delta q_k''$ are back-transformed to the normal coordinates P_i'', Q_i''

$$P_i'' = \sum_k \frac{1}{\sqrt{m_k}} A_{ik}^T \Delta p_k'' \quad (14)$$

$$Q_i'' = \sum_k \sqrt{m_k} A_{ik}^T \Delta q_k'' \quad (15)$$

• **Analytical solution** [propagation by $\exp(\Delta t/2 \hat{L}_{H_0})$]: the normal coordinates are again rotated in phase space for $\Delta t/2$:

$$\begin{bmatrix} P_i \\ Q_i \end{bmatrix} = \mathbf{R} \begin{bmatrix} P_i'' \\ Q_i'' \end{bmatrix} \quad (16)$$

This concludes one full SISIM integration step, which is repeated until the desired number of integration steps is reached.

In this study we used a model MD Hamiltonian⁸

$$H = \sum_i \frac{p_i^2}{2m_i} + \sum_{\text{bonds}} k_b (b - b_0)^2 + \sum_{\text{angles}} k_\vartheta (\vartheta - \vartheta_0)^2 + \sum_{i>j} \frac{e_i e_j}{r_{ij}} + \sum_{i>j} 4\epsilon_{ij} \left[\left(\frac{\sigma_{ij}}{r_{ij}} \right)^{12} - \left(\frac{\sigma_{ij}}{r_{ij}} \right)^6 \right] \quad (17)$$

where i and j run over all atoms, m_i is the mass of the i th atom, \mathbf{p}_i is the linear momentum of the i th atom, b_0 and ϑ_0 are reference values for bond lengths and angles, respectively, k_b and k_ϑ are corresponding force constants, e_i denotes the charge on the i th atom, r_{ij} is the distance between atoms i and j , and ϵ_{ij} and σ_{ij} are the corresponding constants of the Lennard-Jones potential.

The kinetic energy and the harmonic part of the bond stretching and angle bending potential energy of the system in terms of the Cartesian displacement coordinates are included in H_0 , while H_r is the remaining part of the potential. H_0 describes the vibrational motion of the system as well as the translation and rotation of molecules. The motion governed by H_0 is resolved by diagonalizing the Hessian, which is the root-mass-weighted second derivative matrix of the bond stretching and angle bending part of the potential function, to obtain the vibrational frequencies and normal mode vectors of H_0 .¹⁷ The Hessian depends only on the constant parameters of the simulation. This allows the calculation of the vibrational frequencies and normal mode vectors of H_0 to be performed only once, at the beginning of the calculation. Our approach is different from other splitting methods, e.g., Verlet-I/r-RESPA,^{7,15} a multiple time step numerical integration method, in that it analytically treats high-frequency motions using normal modes.¹⁷ Therefore, the SISIM allows a significantly larger integration time step to be used in comparison to standard MD integration methods of the same order and complexity.

3. NUMERICAL RESULTS

The SISIM described here was evaluated on a model system of 256 linear butadiyne molecules of the form $\text{H}-(\text{C}\equiv\text{C}-)_2-\text{H}$. All calculations were performed at three different densities of the system: $\rho_1 = 0.00001 \text{ g/cm}^3$, $\rho_2 = 0.001 \text{ g/cm}^3$, and $\rho_3 = 0.7364 \text{ g/cm}^3$. The densities ρ_1 and ρ_2 correspond to the gas phase, and ρ_3 corresponds to the experimental density of the liquid at 300 K.¹⁸ The corresponding sizes of the simulation box were 1284 Å, 277 Å, and 31 Å, respectively. The initial positions and velocities of the system atoms were chosen at random. Then the system was equilibrated for 50 ps during which the velocities were scaled, followed by an additional 200 ps of the microcanonical equilibration run to ensure that the velocities at a temperature of 300 K assume a Maxwell distribution.

To obtain physically and numerically relevant initial conditions to perform the MD simulation of a system of

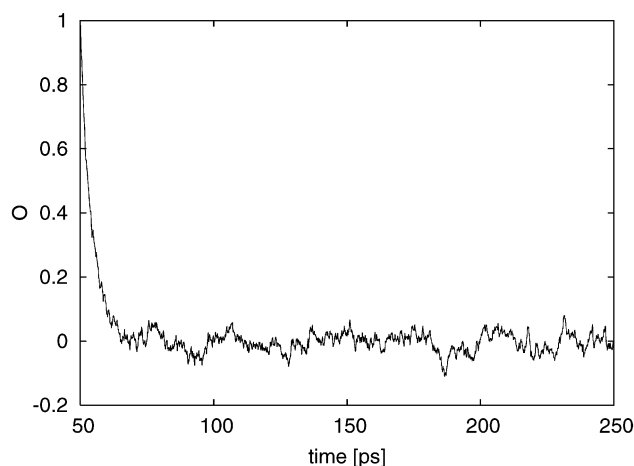


Figure 2. Variation of Viellard-Baron rotational order parameter for linear molecules during the microcanonical equilibration phase of a molecular dynamics simulation of the system of 256 butadiyne molecules at the system density of $\rho_3 = 0.7364 \text{ g/cm}^3$.

linear molecules, the equilibration was also monitored using the Viellard-Baron rotational order parameter for linear molecules¹⁹ defined as

$$O = \frac{1}{n} \sum_{i=1}^n \cos \gamma_i \quad (18)$$

where γ_i is the angle between the current direction of the molecular axis of the i th molecule and the original direction at the beginning of the 200 ps long microcanonical equilibration, and n is the number of molecules in the system. Figure 2 shows that the order parameter drops from the initial value of one to zero during the equilibration of a system of butadiyne molecules at the system density $\rho_3 = 0.7364 \text{ g/cm}^3$. This indicates that the molecules are completely rotationally disordered and that the liquid state has been reached at equilibrium. The initial conditions obtained in this way were used in all of our computations.

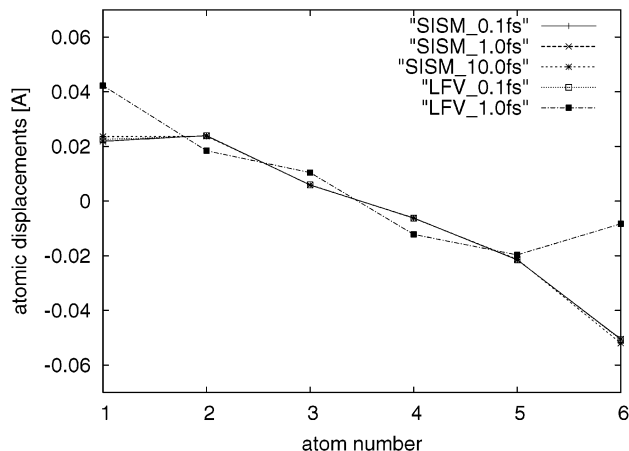
Periodic boundary conditions were imposed to overcome the problem of surface effects; the minimum image convention was used.¹ The Coulomb interactions were truncated using force-shifted potential with a cutoff distance of $r_{\text{off}} = 8.5 \text{ \AA}$.²⁰ The Lennard-Jones interactions were shifted by adding the term $C_{ij}r_{ij}^6 + D_{ij}$ to the potential, where C_{ij} and D_{ij} were chosen such that the potential and force are zero at $r_{ij} = r_{\text{off}}$.²¹ Potential parameters were the same as those taken in ref 11.

To demonstrate the effectiveness of the SISIM, we compared the computational performances for the same level of accuracy with the standard second-order LFV algorithm.¹³

First, the CPU times for the two methods (the SISIM and LFV) for 1000 MD steps measured on an AMD Athlon XP 1600+ processor²² for different system sizes (n) and equal time steps (1 fs) are given in Table 1. The results show that the computation cost per integration step is slightly larger for the SISIM than for the LFV. For larger system sizes the cost of computation per integration step becomes approximately the same for both methods because the computation of long-range forces, which is the same for both methods, prevails over the computation of extra transformations required by the SISIM. Therefore the speed up of the

Table 1: CPU Time [s] for SISM and LFV for 1000 MD Steps Measured on an AMD Athlon XP 1600+ Processor for Different System Sizes (n) and Equal Integration Time Steps (1 fs)

n	$t(\text{SISM})[\text{s}]$	$t(\text{LFV})[\text{s}]$	$t(\text{SISM})/t(\text{LFV})$
64	28.06	24.31	1.15
128	94.56	86.41	1.09
256	339.85	322.98	1.05

**Figure 3.** Displacements of atoms from equilibrium positions for an isolated molecule of butadiyne after 1 ps of simulation at $T = 300$ K computed by SISM and LFV with different integration time step sizes (0.1 fs, 1.0 fs, and 10.0 fs).

SISM over the LFV is mainly due to the larger integration time step allowed by the SISM.

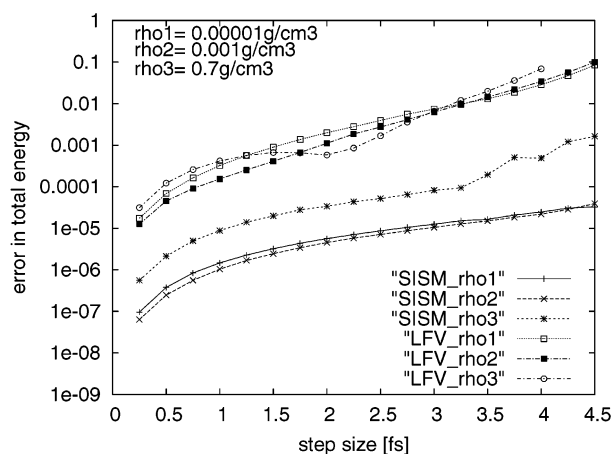
Second, the displacements of atoms from equilibrium positions were computed for an isolated butadiyne molecule in the z direction of the Cartesian coordinate system after a 1 ps long simulation. The atomic displacements were computed by the SISM and LFV with different sizes of the integration time step (0.1 fs, 1.0 fs, and 10.0 fs). These atomic displacements are presented in Figure 3. The displacements computed by the SISM with a 0.1 fs integration time step were used as the reference in the comparison with the displacements computed with different methods and/or sizes of the integration time step. Figure 3 shows that the displacements computed using the SISM agree for all integration time step sizes. The displacements computed by the LFV method, on the contrary, differ from the reference values even in the case of a 1.0 fs integration time step, especially for hydrogen atoms. This means that the SISM, owing to the analytical treatment of high-frequency vibrations, can correctly describe the atomic displacements using a large integration time step, as opposed to the LFV method.

Third, the error in total energy, $\Delta E/E$, defined as

$$\frac{\Delta E}{E} = \frac{1}{M} \sum_{i=1}^M \frac{|E_0 - E_i|}{E_0} \quad (19)$$

where E_0 is the initial energy, E_i is the total energy of the system at the integration step i , and M is the total number of integration steps, was also monitored for both methods.

Figure 4 shows the error in total energy of the model system of butadiyne molecules for three different system densities ($\rho_1 = 0.00001$ g/cm³, $\rho_2 = 0.001$ g/cm³, and $\rho_3 = 0.7364$ g/cm³) using the LFV and SISM algorithms for $M = 1000$. It can be observed that for the same level of

**Figure 4.** Error in total energy of the system of 256 molecules of butadiyne for three different densities of the system: $\rho_1 = 0.00001$ g/cm³, $\rho_2 = 0.001$ g/cm³, and $\rho_3 = 0.7364$ g/cm³ using SISM and LFV for $M = 1000$.

accuracy, the SISM allows the use of an up to an order of magnitude larger integration time step than the LFV. The maximal integration time step allowed is only 0.5 fs for all three densities ρ_1 , ρ_2 , and ρ_3 in the case of the LFV, while it is 4.5 fs for ρ_1 and ρ_2 and 3.0 fs for ρ_3 in the case of the SISM. With the growing density of the system the maximal allowed integration time step by the SISM becomes shorter due to the Lennard-Jones and electrostatic interactions which are treated numerically, equally, in both methods. The Lennard-Jones and electrostatic interactions represent the external driving forces on the internal motion of the molecules. The effect of the Lennard-Jones and electrostatic interactions is reflected in the forced oscillations and increased anharmonicity in the case of the denser system, which leads to a shortening of the integration time step.

Fourth, to determine the dependence of the quality of the harmonic approximation for the bond stretching and angle bending potential on the system density, we introduced a measure for the anharmonicity in the bonding potential energy, defined as

$$A_n = \frac{1}{M} \sum_{i=1}^M \times \frac{\left| \sum_{\text{bonds}} k_b (b - b_0)^2 + \sum_{\text{angles}} k_\theta (\vartheta - \vartheta_0)^2 - \frac{1}{2} \sum_{j=1}^n \sum_{k=1}^{3N} \omega_k^2 Q_{k_j}^2 \right|}{\frac{1}{2} \sum_{j=1}^n \sum_{k=1}^{3N} \omega_k^2 Q_{k_j}^2} \quad (20)$$

Here, M is the total number of integration steps, n is the number of molecules, and N is the number of atoms in each molecule. The numerator in (20) represents the difference at the integration time step i between the whole bonding potential energy and the pure harmonic potential energy as expressed by the normal coordinates. The denominator in (20) is the pure harmonic potential energy.

The results presented in Figure 5 reveal that the anharmonic part of the bonding potential energy depends only on the density of the system and not on the size of the integration time step. From the results in Figure 5 it can also be

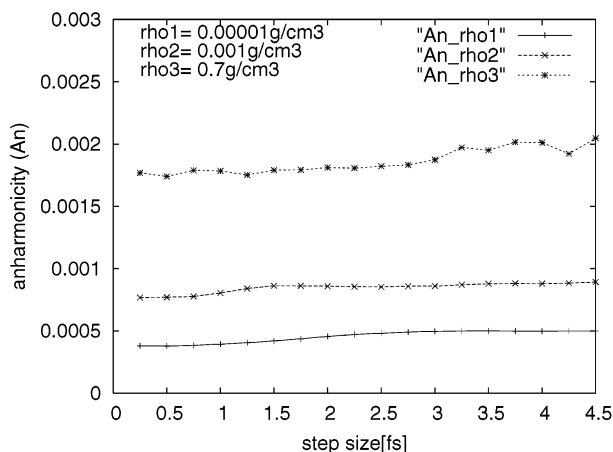


Figure 5. Amount of anharmonicity in the bonding potential energy (A_n) for the system of 256 molecules of butadiyne for three different densities of the system: $\rho_1 = 0.00001 \text{ g/cm}^3$, $\rho_2 = 0.001 \text{ g/cm}^3$, and $\rho_3 = 0.7364 \text{ g/cm}^3$ computed by SISIM for $M = 1000$.

Table 2: Average of Quotients of Magnitudes of Harmonic and Anharmonic Forces Acting on Atoms of the System of 256 Butadiyne Molecules for Three Different Densities of the System: $\rho_1 = 0.00001 \text{ g/cm}^3$, $\rho_2 = 0.001 \text{ g/cm}^3$, and $\rho_3 = 0.7364 \text{ g/cm}^3$ Computed by SISIM for $M = 1000$ Using $\Delta t = 0.5 \text{ fs}$ and $\Delta t = 3.0 \text{ fs}$ Integration Time Steps

ρ	$Avg[\Delta t = 0.5 \text{ fs}]$	$Avg[\Delta t = 3.0 \text{ fs}]$
$\rho_1 = 0.00001 \text{ g/cm}^3$	32.17	30.95
$\rho_2 = 0.001 \text{ g/cm}^3$	30.72	30.31
$\rho_3 = 0.7364 \text{ g/cm}^3$	14.50	14.73

concluded that as the density of the system increases the quality of the harmonic approximation for the bond stretching and angle bending potential in terms of the Cartesian displacement coordinates deteriorates.

Fifth, to study the influence of the system density on the size of the integration time step allowed by the SISIM, we computed the average of the quotients (Avg) of the magnitude of the harmonic and the anharmonic forces acting on an atom of the system. This quotient, which is averaged over all the atoms of the system and the total number of integration steps, is defined as

$$Avg = \frac{1}{M} \sum_{i=1}^M \left\langle \frac{|F_{\text{harm}}|}{|F_{LJ} + F_{\text{elec}} + F_{\text{bonds+angles}} - F_{\text{harm}}|} \right\rangle_i \quad (21)$$

where M is the total number of integration steps and $\langle \cdot \rangle$ represents the averaging over all the atoms of the system. The numerator in (21) represents the magnitude of the harmonic force acting on an atom of the system at the integration step i . The harmonic force is derived from the harmonic part of the bond stretching and angle bending potential energy in terms of the Cartesian displacement coordinates. The denominator in (21) is the harmonic force subtracted from the total force acting on an atom of the system due to the Lennard-Jones, electrostatic, bond stretching, and angle bending potentials, respectively. This difference represents the total anharmonic force computed in the numerical part of the SISIM, which generates atoms' motion that limits the size of the integration time step. The results given in Table 2 reveal that the bonded harmonic forces within molecules are an order of magnitude greater than the anharmonic forces in the system at all system densities.

However, as the density of the system increases, the magnitude of the anharmonic forces acting on the system atoms also increases, and therefore the size of the integration time step allowed by the SISIM becomes smaller but remains significantly larger than possible by the LFV.

4. CONCLUSIONS

In this paper the study of the system density dependence of the size of the maximal allowed integration time step by the Split Integration Symplectic Method (SISIM) for MD integration was presented. The numerical results of a model system of 256 butadiyne molecules showed that as the density of the system increases, the magnitude of anharmonic intermolecular electrostatic and van der Waals forces acting on the system atoms also increases, and therefore the size of the integration time step, which is limited by the atoms' motion generated by the intermolecular forces in the case of the SISIM, becomes smaller. The maximal integration time step allowed by the standard leapfrog Verlet (LFV) method, however, does not depend on the system density because it is limited by the high-frequency vibrations of the atoms within every molecule of the system. Since the time scale for intramolecular motion is considerably smaller than the time scale corresponding to the motion generated by the intermolecular forces regardless of the system density, the SISIM allows an integration time step significantly larger than can be used by the standard LFV method, while retaining the same level of accuracy.

ACKNOWLEDGMENT

The authors express their thanks to Drs. Milan Hodošček and Franci Merzel for stimulating discussions as well as to Urban Borštnik for careful reading of the manuscript. This work was supported by the Ministry of Education, Science and Sports of Slovenia under Grant No. P1-104-503.

REFERENCES AND NOTES

- (1) Allen, M. P.; Tildesley, D. J. *Computer Simulation of Liquids*; Clarendon Press: Oxford, 1987.
- (2) Zhang, G.; Schlick, T. LIN: A New Algorithm to Simulate the Dynamics of Biomolecules by Combining Implicit-Integration and Normal Mode Techniques. *J. Comput. Chem.* **1993**, *14*, 1212–1233.
- (3) Izaguirre, J. A.; Reich, S.; Skeel, R. D. Longer Time Steps for Molecular Dynamics. *J. Chem. Phys.* **1999**, *110*, 9853–9864.
- (4) Skeel, R. D.; Zhang, G.; Schlick, T. A Family of Symplectic Integrators: Stability, Accuracy, and Molecular Dynamics Applications. *SIAM J. Sci. Comput.* **1990**, *18*, 203–222.
- (5) Schlick, T.; Barth, E.; Mandziuk, M. Biomolecular Dynamics at Long Timesteps: Bridging the Timescale Gap between Simulation and Experimentation. *Annu. Rev. Biophys. Biomol. Struct.* **1997**, *26*, 181–222.
- (6) Tuckerman, M. E.; Martyna, G. J.; Berne, B. J. Molecular Dynamics Algorithm for Condensed Systems with Multiple Time Scales. *J. Chem. Phys.* **1990**, *93*, 1287–1291.
- (7) Tuckerman, M. E.; Berne, B. J.; Martyna, G. J. Reversible Multiple Time Scale Molecular Dynamics. *J. Chem. Phys.* **1992**, *97*, 1990–2001.
- (8) Sanz-Serna, J. M.; Calvo, M. P. *Numerical Hamiltonian Problems*; Chapman & Hall: London, 1994.
- (9) Janežič, D.; Merzel, F. An Efficient Symplectic Integration Algorithm for Molecular Dynamics Simulations. *J. Chem. Inf. Comput. Sci.* **1995**, *35*, 321–326.
- (10) Janežič, D.; Merzel, F. Split Integration Symplectic Method for Molecular Dynamics Integration. *J. Chem. Inf. Comput. Sci.* **1997**, *37*, 1048–1054.
- (11) Janežič, D.; Praprotnik, M. Symplectic Molecular Dynamics Integration using Normal Mode Analysis. *Int. J. Quantum Chem.* **2001**, *84*, 2–12.

- (12) Praprotnik, M.; Janežič, D. The Split Integration Symplectic Method. *Cell. Mol. Biol. Lett.* **2002**, *7*, 147–148.
- (13) Verlet, L. Computer “Experiments” on Classical Fluids. I. Thermodynamical Properties of Lennard-Jones molecules. *Phys. Rev.* **1967**, *159*, 98–103.
- (14) Goldstein, H. *Classical Mechanics*, 2nd ed.; Addison-Wesley Publishing Company: Reading, 1980.
- (15) Grubmueller, H.; Heller, H.; Windemuth, A.; Schulten, K. Generalized Verlet Algorithm for Efficient Molecular Dynamics Simulations with Long-Range Interactions. *Mol. Sim.* **1991**, *6*, 121–142.
- (16) Bright Wilson, E., Jr.; Decius, J. C.; Cross, P. C. *Molecular Vibrations*; McGraw-Hill Book Company, Inc.: New York, 1955.
- (17) Brooks, B. R.; Janežič, D.; Karplus M. Harmonic Analysis of Large Systems: I. Methodology. *J. Comput. Chem.* **1995**, *16*, 1522–1542.
- (18) Weast, R. C., Ed.; *CRC Handbook of Chemistry and Physics*, 66th ed.; CRC Press Inc.: Cleveland, 1986.
- (19) Vieillard-Baron, J. E. Phase Transitions of The Classical Hard Ellipse System. *J. Chem. Phys.* **1972**, *56*, 4729–4744.
- (20) Prevost, M.; van Belle, D.; Lippens, G.; Wodak, S. Computer Simulations of Liquid Water: Treatment of Long-Range Interactions. *Mol. Phys.* **1990**, *71*, 587–603.
- (21) Steinbach, P. J.; Brooks, B. R. New Spherical-Cutoff Methods for Long-Range Forces in Macromolecular Simulation. *J. Comput. Chem.* **1994**, *15*, 667–683.
- (22) Hodošček, M.; Borštnik, U.; Janežič, D. CROW for large scale macromolecular simulations. *Cell. Mol. Biol. Lett.* **2002**, *7*, 118–119.

CI034145B